Glycoconj J (2014) 31:209–219
DOI 10.1007/s10719-013-9511-9

Individual profiles of free ceramide species and the constituent ceramide species of sphingomyelin and neutral glycosphingolipid and their alteration according to the sequential changes of environmental oxygen content in human colorectal cancer Caco-2 cells

Kouji Tanaka · Keiko Tamiya-Koizumi · Masaki Yamada · Takashi Murate · Reiji Kannagi · Mamoru Kyogashima

Received: 27 September 2013 / Revised: 1 November 2013 / Accepted: 3 November 2013 / Published online: 6 December 2013

Abstract We previously performed a systematic analysis of free ceramide (Cers) species, the constituent ceramide species of sphingomyelins and neutral glycosphingolipids (NGSLs) using matrix-assisted laser desorption/ionization time-of-flight mass spectrometry with high-energy collision-induced dissociation. As a result, distinct species differences were found among Cers, sphingomyelins and NGSLs in the kidneys. Using this method, we investigated various sphingolipid species from human colon cancer Caco-2 cells as well as the influence of environmental oxygen on these species in detail. Unexpectedly, even in normoxia, all Cers species were composed of dihydrosphingosine (d18:0) and non-hydroxy fatty acid (NFA), and 34 % of sphingomyelins were composed of dihydrosphingomyelins with NFA. In contrast, major constituent ceramide species of NGSLs were composed of the usual long-chain base of sphingosine (d18:1) and hydroxy fatty acid (HFA). When the cells were cultured under hypoxic condition for 3 days, all the Cers and nearly 80 % of the sphingomyelins were dihydrosphingolipids composed of d18:0-NFAs, but a significant proportion of d18:1-HFAs still remained in the NGSLs. When the cells were transferred from conditions of hypoxia to normoxia again (reoxygenation), Cer species composed of d18:1-NFAs, which were not found in Cers under the original normoxic conditions, appeared. Such Cers were probably synthesized as precursors for the constituent ceramides of sphingomyelins and NGSLs.

Keywords 4–6: Ceramides · Sphingomyelins · Glycosphingolipids · Dihydrosphingolipids · Hypoxia · Reoxygenation

Electronic supplementary material The online version of this article (doi:10.1007/s10719-013-9511-9) contains supplementary material, which is available to authorized users.

K. Tanaka · K. Tamiya-Koizumi · T. Murate
Department of Medical Technology, Nagoya University Graduate School of Health Sciences, Daiko-Minami 1-1-20, Higashi-ku, Nagoya 461-8673, Japan

M. Yamada
Shimadzu Corporation, Nishinokyo-Kuwabaracho 1, Nakagyo-ku, Kyoto 604-8511, Japan

R. Kannagi
Research Complex for the Medicine Frontiers, Aichi Medical University, Yazako, Nagakute, Aichi 480-1195, Japan

M. Kyogashima (✉)
Department of Microbiology and Molecular Cell Biology, Nihon Pharmaceutical University, Komuro 10281, Inamachi, Saitama 362-0806, Japan
e-mail: mkyogashi@nichiyaku.ac.jp

Introduction

As glycomics/lipidomics techniques using current mass spectrometry advances [1–3], it has become more important to identify the particular molecular species that exert the specific functions of sphingolipids [1, 4]. For example, the sulfatide containing non hydroxyl fatty acid (NFA) C16:0, but not C24:0, inhibited insulin secretion in rat beta-cells [5], and lactosylceramide (LacCer) possessing C24:0 and C24:1 mediated superoxide generation and migration in neutrophils [6]. In clinics, down-regulation of C18-ceramide (d18:1-C18:0) was associated to lymphovascular invasion in human head and neck squamous cell carcinomas [7]. In addition, the

importance is steadily growing for dihydrosphingolipids containing dihydrosphingosine (d18:0) as a long-chain base. Dihydroceramides (dihydroCers, d18:0-NFAs), which were previously believed to be inert lipids, carry out specific roles in cell growth regulation and autophagy [8, 9], and the age-related increase of dihydrosphingomyelin (d18:0-C16:0) in human lens suggesting an association with the development of cataract [10]. However, there has been few reports on dihydroglycosphingolipids (dihydroGSLs). Moreover, although GSLs containing hydroxyl FAs (HFAs) are abundant in myelin, skin, intestines, and kidneys [11], there has been little investigation of the species containing HFAs and d18:0.

Therefore, to elucidate sphingolipid species comprehensively, we previously performed a systematic analysis of free ceramide species (hereafter, we abbreviate free ceramides including free dihydroceramides as Cers to distinguish them from constituent ceramides) species, the constituent ceramide species of sphingomyelins and neutral GSLs (NGSLs). In the previous study, matrix-assisted laser desorption/ionization time-of-flight mass spectrometry (MALDI-TOF MS) with high-energy collision-induced dissociation, identified distinct species differences among Cers, sphingomyelins and NGSLs in the kidneys [12]. However, the kidneys are composed of numerous cell types such as renal tubule cells, endothelial cells, mesangial cells and podocytes. Therefore, it is uncertain whether these differences in the ceramide species are a reflection of different sphingolipid metabolic pathways working in different cell types or different metabolism of individual classes of sphingolipids.

Here, using human colon cancer cell lines Caco-2, we performed systematic analysis of diverse species of various types of sphingolipids. Furthermore, we investigated the influences of hypoxia and subsequent reoxygenation on oxygen molecule required sphingolipid metabolism. Previously, the influence of hypoxia on Cer and sphingomyelins has been reported in breast cancer cells [13], but detailed analysis has not been carried out on the influence of hypoxia and subsequent reoxygenation on sphingolipids including GSLs. In this study, the dynamics of sphingolipid metabolism from Cers to sphingomyelins and GSLs are investigated along with the time course of normoxia, hypoxia and reoxygenation.

Materials and methods

Cells and hypoxic culture

Caco-2 cells were from the American Type Culture Collection (Manassas, VA). Cells were cultured in DMEM (Invitrogen, Carlsbad, CA) supplemented with 10 % fetal calf serum at 37 °C with CO_2 (5 %) and O_2 (20 %) for 3 days (normoxia). For hypoxia experiment, after 1 day of culture under a normoxic condition, the cells were transferred to a condition of 37 °C with CO_2 (5 %) and O_2 (1 %) in a multi-gas incubator (Juji Field, Inc., Tokyo, Japan), and continuously cultured for 3 days. For reoxygenation, after 3 days under the hypoxic condition, the cells were transferred to newly prepared culture media and continuously cultured under normoxia for a further 12 or 24 h.

Preparations of Cers, sphingomyelins and NGSLs

Sphingolipids were purified from 5.0×10^7 cells as previously described [12]. Briefly, lipids were extracted with a chloroform–methanol mixture. Using Florisil (Wako, Osaka, Japan) column chromatography, NGSLs including HexCers, Hex2Cers, Hex3Cers and HexNAc(Hex)3Cer in the Folch lower phase were completely separated by the acetylation/deacetylation method from phospholipids such as alkali resistant ether-linked glycerophospholipids and sphingomyelin [14]. Cers and sphingomyelins were prepared by preparative thin-layer chromatography (TLC). The solvent mixtures used for sphingomyelins, and Cers were chloroform:methanol:H_2O (65:25:4 by volume) and chloroform:methanol:acetic acid (95:1:4), respectively. Cers including phytosphingosine with NFAs/HFAs were separated completely by the solvent and recoveries of various molecular species of Cers and sphingomyelins were sufficient at qualitative and quantitative levels as described previously (12, 15).

MALDI-TOF MS, MS/MS

Mass spectrometry was performed as previously described [12]. Lipids were prepared as 10–350 pmol/μl solutions in chloroform:methanol (2:1). One microliter each of matrix (10 mg/ml 2,5-dihydroxybenzoic acid in chloroform:methanol (2:1) with or without 0.5 % trifluoroacetic acid and lipid solution were mixed vigorously and 1 μl of the resultant solution was applied onto the surface of a stainless steel MALDI-TOF plate. Analyses were performed in positive ion mode using an AXIMA-Performance mass spectrometer (Shimadzu/Kratos,UK) equipped with a nitrogen UV laser (337 nm). The instrument was operated at an acceleration voltage of 20 keV and a pulsed extraction function to improve mass resolution was carefully applied to the m/z range of 400–1600, based on the sizes of the target molecules. The TOF analyzer was calibrated using the following external calibrants: a dimer of α-cyano-4-hydroxycinnamic acid ($[2\ M + H]^+$; 379.09), human angiotensin II ($[M + H]^+$; 1046.54), and ACTH18–39 ($[M + H]^+$; 2465.20). Helium gas was used for high-energy CID (20 keV) fragmentation for MS/MS analysis. All mass spectrometric data were acquired and analyzed using MALDI-MS software (Shimadzu/Kratos). The compositions of molecular species from each class of lipid were calculated from the peak areas obtained from spectra as previously described [12].

Results and discussion

Linear mode and MS/MS analyses of Cers and sphingomyelins

Figure 1 shows the linear mode mass spectra of Cers from Caco-2 cells under normoxia (Fig. 1a), hypoxia (Fig. 1b) and reoxygenation at 12 (Fig. 1c) and 24 h (Fig. 1d). As we previously reported, in MALDI-TOF MS, the major molecular ions of typical Cers of d18:1-FAs were detected as $[M + H - H_2O]^+$ and $[M + Na]^+$, and dihydroCers of d18:0-FAs were detected as $[M + H]^+$ and $[M + Na]^+$, because of the high sensitivity to dehydration caused by the trans-double bond in the long-chain base [12]. From the cells under a

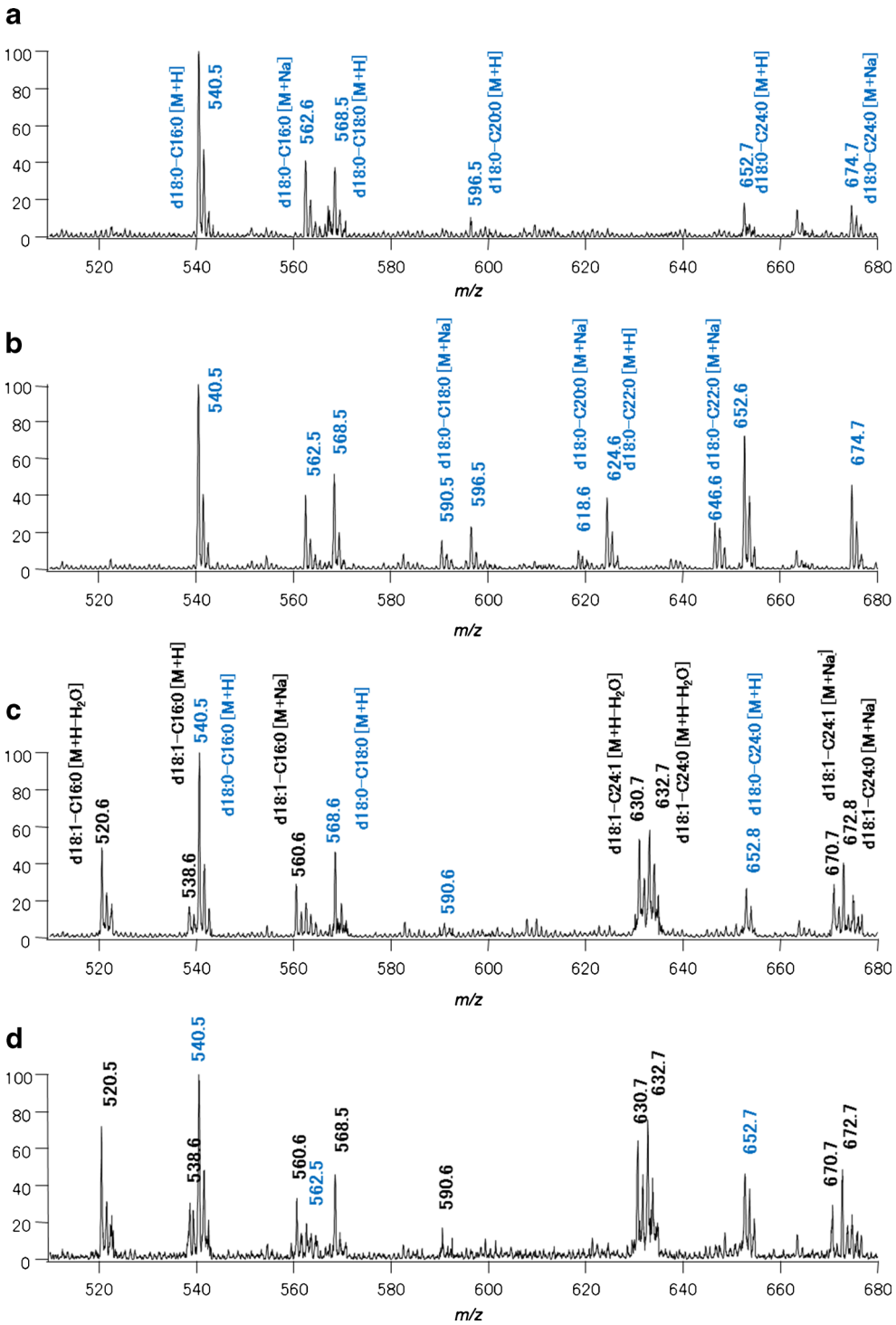

Fig. 1 Linear mode mass spectra of Cers. Normoxia (**a**), hypoxia (**b**), reoxygenation for 12 h (**c**), and reoxygenation for 24 h (**d**); black and blue letters indicate ions from Cer with d18:1 and Cer with d18:0 (dihydroceramide) species, respectively

normoxic condition, ions at *m/z* 540.5 ($[M + H]^+$, d18:0-C16:0), 562.5 ($[M + Na]^+$, d18:0-C16:0), 568.5 ($[M + H]^+$, d18:0-C18:0), 596.5 ($[M + H]^+$, d18:0-C20:0), 652.7 ($[M + H]^+$, d18:0-C24:0), and 674.7 ($[M + Na]^+$, d18:0-C24:0) were detected, surprisingly indicating that the Cers of the Caco-2 cells were composed of dihydroCers, even under normoxia. MS/MS analyses were performed (see Supplemental Fig. 1a) and the above ions were confirmed as being from dihydroCers. There were no dihydroCer species with C24:1 as the fatty acid. From the cells under hypoxic conditions for 3 days, in addition to the ions observed under normoxia, ions at *m/z* 590.5 ($[M + Na]^+$, d18:0-C18:0), 618.6 ($[M + Na]^+$, d18:0-C20:0), 624.6 and 646.7 ($[M + H]^+$ and $[M + Na]^+$, d18:0-C22:0) were detected and the peaks of ions at m/z 652.6 and 674.7 became relatively more intense. From the cells reoxygenated for 12 and 24 h, the ions corresponding to d18:0-C20:0 and d18:0-C22:0 disappeared but ions at *m/z* 520.6 ($[M + H - H_2O]^+$, d18:1-C16:0), 538.6($[M + H]^+$, d18:1-C16:0, 560.6 ($[M + Na]^+$, d18:1-C16:0), 630.7 ($[M + H - H_2O]^+$, d18:1-C24:1), 632.7 ($[M + H - H_2O]^+$, d18:1-C24:0), 670.7 ($[M + Na]^+$, d18:1-C24:1), and 672.8 ($[M + Na]^+$, d18:1-C24:0) appeared.

Figure 2 shows the linear mode mass spectra of sphingomyelins from Caco-2 cells. Under normoxia (Fig. 2a) and hypoxia (Fig. 2b), ions were detected at *m/z* 703.6 ($[M + H]^+$, d18:1-C16:0), 725.7 ($[M + Na]^+$, d18:1-C16:0), 705.8 ($[M + H]^+$, d18:0-C16:0), 727.7 ($[M + Na]^+$, d18:0-C16:0), 733.8 ($[M + H]^+$, d18:0-C18:0), 755.9 ($[M + Na]^+$, d18:0-C18:0), 761.9 ($[M + H]^+$, d18:0-C20:0), 787.8 ($[M + H]^+$, d18:1-C22:0), 789.9 ($[M + H]^+$, d18:0-C22:0), 811.7 ($[M + Na]^+$, d18:0-C22:0), 813.8 ($[M + H]^+$, d18:1-C24:1), 835.8 ($[M + Na]^+$, d18:1-C24:1), 815.8 ($[M + H]^+$, d18:1-C24:0), 837.8 ($[M + Na]^+$, d18:1-C24:0), 817.9 ($[M + H]^+$, d18:0-C24:0), and 839.9 ($[M + Na]^+$, d18:0-C24:0). The protonated ions were analyzed by MS/MS and a product ion *m/z* at 184.4 was confirmed, which is specific for lipids containing phosphocholine (see Supplemental Fig. 1b) [3]. Unlike Cers, the major long-chain base was d18:1 (66 %), with a relatively high proportion of dihydrosphingosine d18:0 (34 %). It should be noted that d18:0 was the only detected sphingomyelin with C16:0 and not in those with C22:0 C24:1 and C24:0. Under the hypoxia, species with d18:0 became the majority as expected.

Linear mode and MS/MS analyses of HexCers, and Hex3Cers

Figure 3 shows the linear mode mass spectra of HexCers from Caco-2 cells. From the cells under normoxic (Fig. 3a) and hypoxic (Fig. 3b) conditions, ions were detected at *m/z* 722.6 ($[M + Na]^+$, d18:1-C16:0), 738.3 ($[M + Na]^+$, d18:1-C16:0h), 848.5 ($[M + Na]^+$, d18:1-C24:1h), 850.5 ($[M + Na]^+$, d18:1-C24:0h). These are all sodiated ions, no protonated ions were observed, which is consistent with the results from the analysis of GSLs using this MS technique [12]. Hereafter, "$[M + Na]^+$" is omitted in the description of the MS analysis of GSLs. Under hypoxia, among species containing C16, an ion at *m/z* 722.7 derived from d18:1-C16:0 became more intense than the ion observed at *m/z* 738.7 from d18:1-C16:0h and an ion at 722.7 from d18:0-C16:0 was also detected. In contrast, among the species containing C24, ions at m/z 834.8, 836.8, 850.8, and 852.8 from d18:1-C24:0, d18:0-C24:0, d18:1-C24:0h, and d18:0-C24:0h, respectively, became prominent in this order, and the ion at *m/z* 848.5 from d18:1-C24:1, which is the most intense peak under the normoxia, became the least intense under hypoxia. In addition to these ions, ions at *m/z* 808.7 and 824.8 from d18:0-C22:0 and d18:0-C22:0h were detected under hypoxia. After reoxygenations, ions from d18:0-C16:0 and d18:0-C24:0h became time-dependently less prominent with the concomitant prominence of ions from d18:1-C24:0h, d18:1-C24:0, and d18:1-C24:1. The intensity of ions from HexCer (d18:1-C24:1h) increased, but did not return to the level observed under normoxia, after reoxygenation for 24 h (Fig. 3c and d).

Figure 4 shows the linear mode mass spectra of the Hex3Cers from Caco-2 cells. Under normoxia, ions were detected at *m/z* 1046.5, 1048.5, 1062.5, 1064.5, 1130.7, 1132.8, 1146.7, 1156.8, 1158.7, 1160.7, 1172.7, 1174.7, and 1176.8 from d18:1-C16:0, d18:0-C16:0, d18:1-C16:0h, d18:0-C16:0h, d18:1-C22:0, d18:0-C22:0, d18:1-C22:0h, d18:1-C24:1, d18:1-C24:0, d18:0-C24:0, d18:1-C24:1h, d18:1-C24:0h and d18:0-C24:0h, respectively. The constituent ceramide species from HexCers and Hex3Cers were similar. However, a marked proportional difference was observed in hypoxia; in HexCers, an ion from d18:0-C24:0h was the most prominent, whereas in Hex3Cers, the most prominent ion was from d18:0-C24:0. This was confirmed by MS/MS analysis that revealed the characteristic ion of Hex3Cer with d18:0 at *m/z* 864.2 (Fig. 5). As reoxygenation advanced, the signals caused by ions from species of d18:1 became more intense. However in Hex3Cers ions from species with C24:1h and C24:0h remained still minor components and the ions from species with C24:1 and C24:0 (and C22:0), which were not prominent in HexCers, were in the majority.

Compositional comparison of ceramides species of Cers, sphingomyelins and NGSLs, under normoxia, hypoxia and after reoxygenation for 12 and 24 h

As we have previously demonstrated [12, 15, 16], the lipid portions of sphingolipids are much more diverse than commonly thought, because they can be modified with saturation/desaturation, hydroxylation and a different alkyl-chain length. Current lipidomics technique are developing partly conjunction with emergence of many chemically synthesized

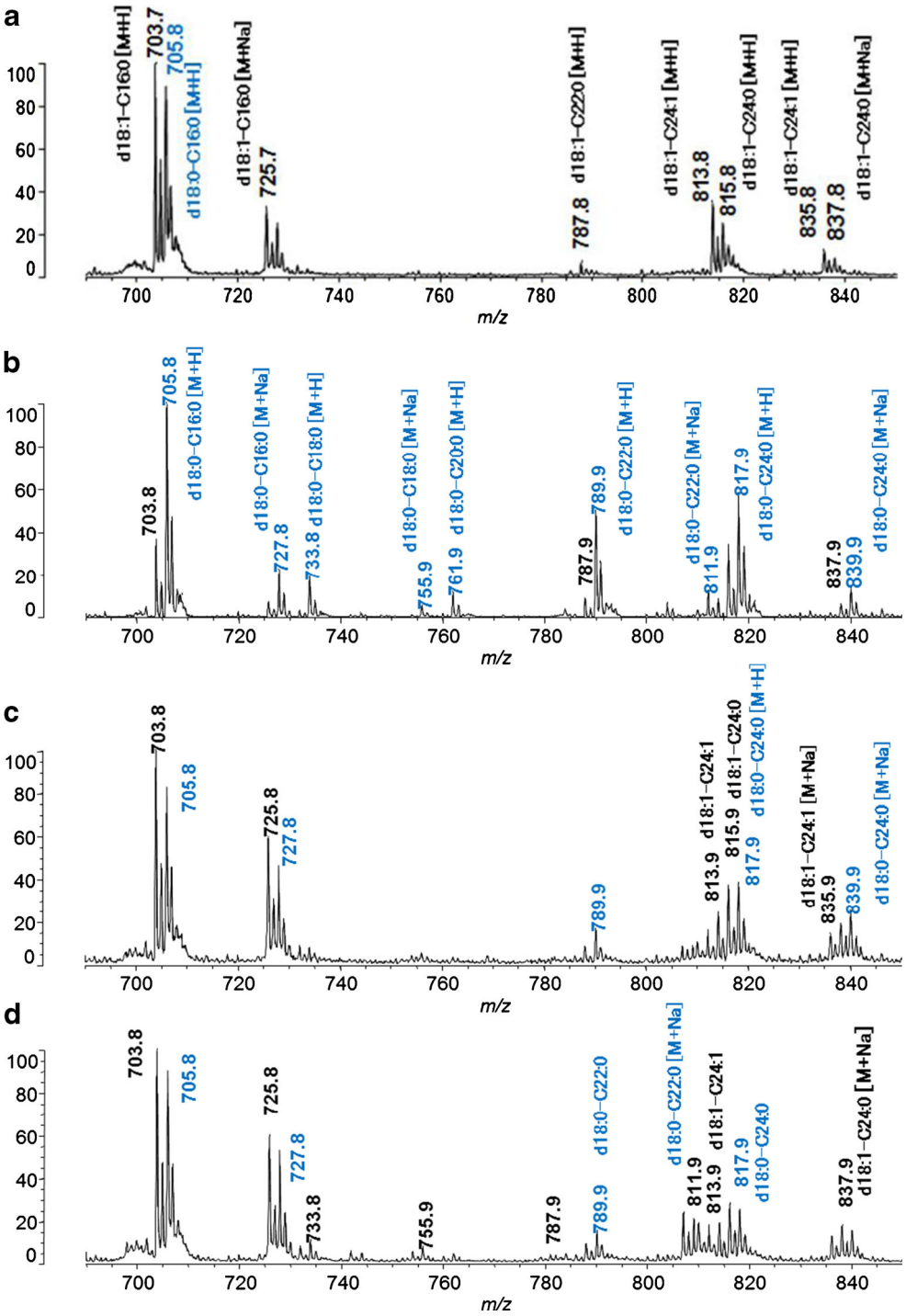

Fig. 2 Linear mode mass spectra of sphingomyelins. Normoxia (**a**), hypoxia (**b**), reoxygenation for 12 h (**c**), and reoxygenation for 24 h (**d**); black and blue letters indicate ions from sphingomyelin and dihydrosphingomyelin species, respectively

molecular species as standards [1, 17]. However, GSLs, especially those expressed in epithelial cells, are often hydroxylated at FAs and/or long-chain bases, causing enormous complexity for MS analysis, because of their heterogeneity in terms of both the carbohydrate and the lipid portion, and lack of verified standards. Consequently, there are still few comprehensive analyses of Cers, sphingomyelins, and GSLs with a longer sugar chain of more than three hexose residues. Therefore, we investigated this subject using a recently developed MALDI-TOF MS/MS system. We summarized the relative ceramide compositions of the Cers, sphingomyelins and NGSLs calculated based on the peak areas of the linear mass profiles (Fig. 6) for an instant overview of the metabolism of sphingolipids [12].

To our surprise, in Caco-2 cells under normoxia, all Cer species contained d18:0 as the long-chain base

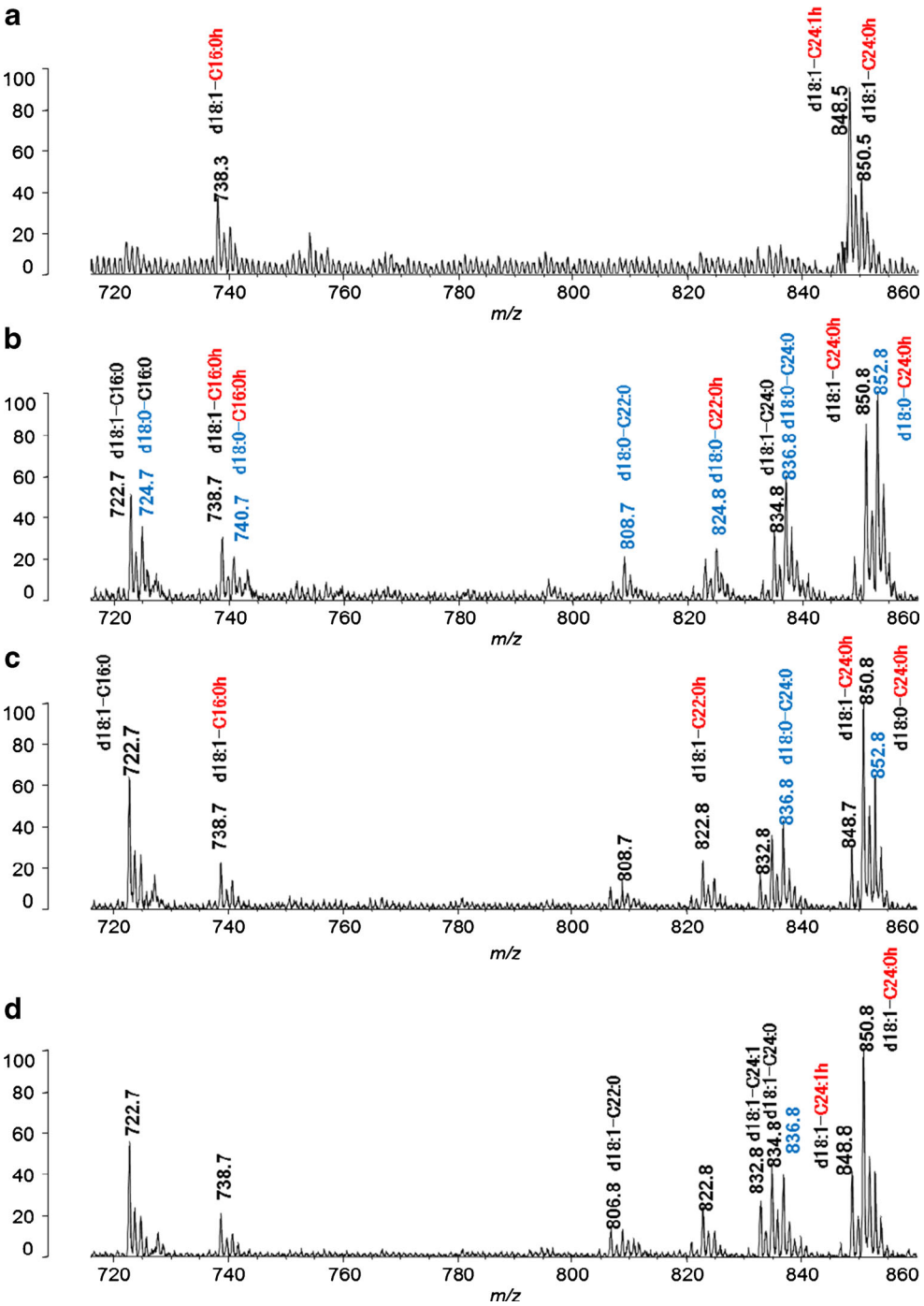

Fig. 3 Linear mode mass spectra of HexCers. Normoxia (**a**), hypoxia (**b**), reoxygenation for 12 h (**c**), and reoxygenation for 24 h (**d**); black and blue letters indicate ions from HexCer with d18:1 and HexCer with d18:0 species, respectively. Red letters indicates species with HFA. All ions are sodiated ions

(Fig. 7 left column). A high proportion of d18:0 was also observed in sphingomyelin with C16:0. A high proportion of dihydrosphingomyelins has been reported to occur in various tumors including colon cancers [18, 19]. Generally cancer cells are resistant to hypoxia [20]. Therefore a high proportion of dihydrosphingomyelins even in the normoxic condition may be advantageous for adaptation to a hypoxic environment. DihydroCer, which was previously considered an inert lipid, is now recognized as a mediator for autophagy [8, 9].

NGSLs of Caco-2 cells were composed of HexCers, Hex2Cers (LacCers), Hex3Cers (Gb3Cers) and HexNAcHex3Cers (Gb4Cers) as previously described [21]. In contrast with Cers and sphingomyelins, the major long-chain base of NGSLs is d18:1 (Fig. 7, left column), suggesting that the cells provides d18:1 priorly for GSLs; then for sphingomyelins and last for Cers, which is consistent with the results of our very early analyses of sphingolipids from human pathological platelets [22]. Another characteristic

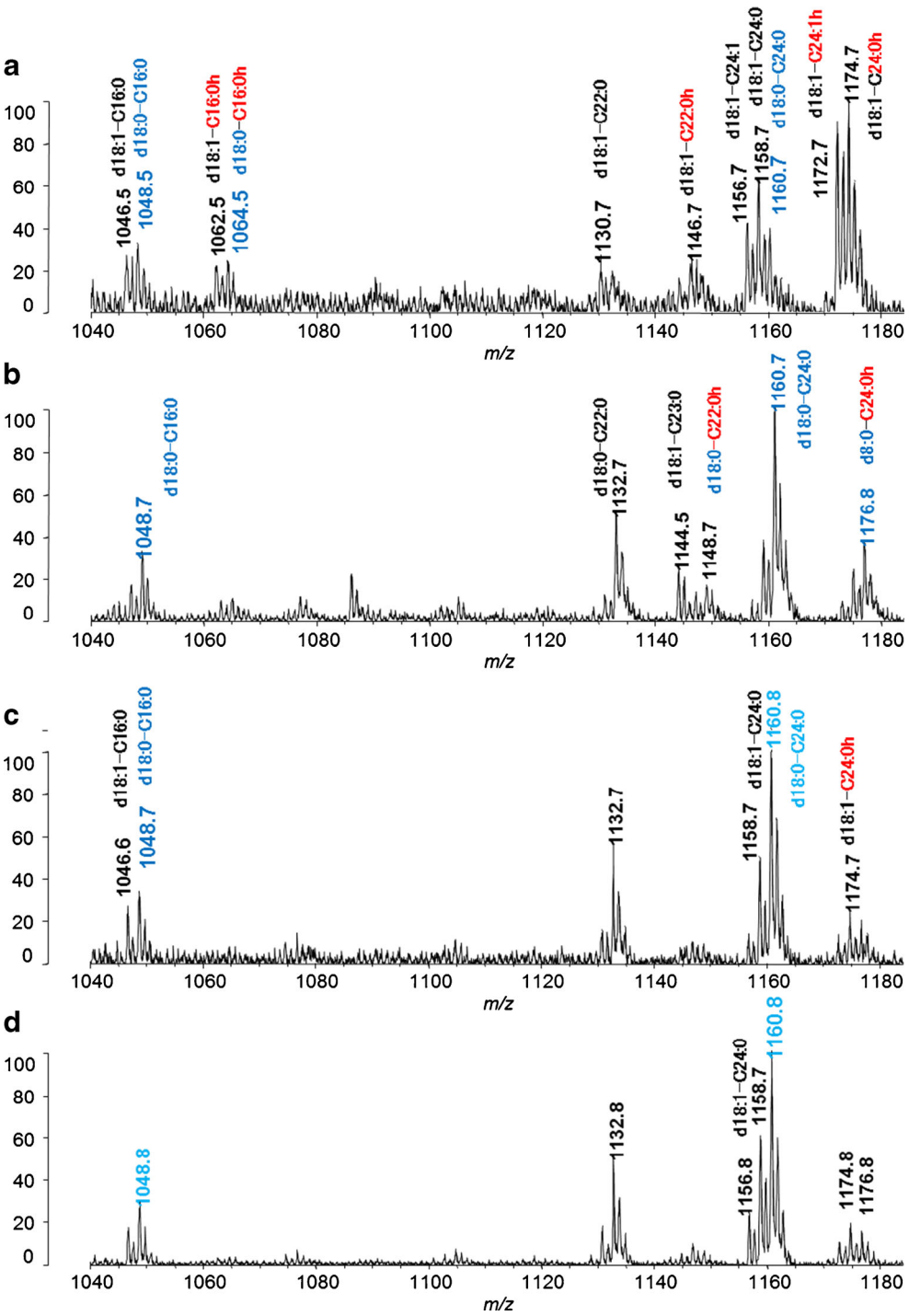

Fig. 4 Linear mode mass spectra of Hex3Cers. Normoxia (**a**), hypoxia (**b**), reoxygenation for 12 h (**c**), and reoxygenation for 24 h (**d**); black and blue letters indicate ions from Hex3Cer with d18:1 and d18:0 species, respectively. Red letters indicate species with HFA. All ions are sodiated ions

property of the constituent ceramides of GSLs is the predominance of HFA, which is particularly remarkable in the short sugar chain of HexCers (72 %) and Hex2Cers (73 %) (Fig. 7, right column). Before MS analysis, we screened for the occurrence of Cers with HFAs using TLC as previously reported [12]. However, no substantial amount of Cers with HFAs was detected in any of the culture conditions investigated. This is consistent with a previous report that the level of Cers with HFA was only 1–3 % of the total Cers [11]. It is likely that synthesized Cers containing HFAs are immediately converted to GSLs in the Caco-2 cells and this may contribute to cell survival. The effect of Cers containing HFAs on the cell fate is a subject of controversy. We have previously shown that exogenous addition of Cers with HFAs (d18:1-HFAs types) produces more cytotoxic effect on human leukemic cells, HL60, K562 and neuroblastoma cells SH-SY5Y than typical

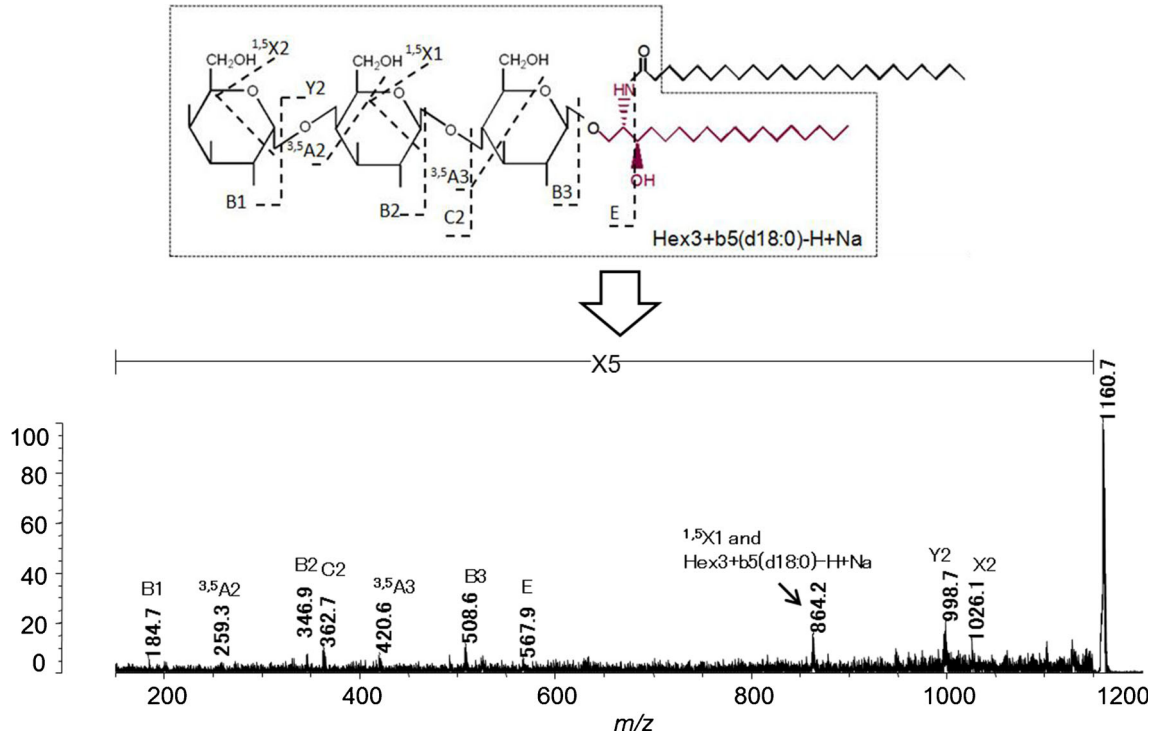

Fig. 5 Fragmentation scheme (*upper*) and MS/MS profile of the $[M + Na]^+$ ion at *m/z* 1160.7 derived from Hex3Cer with d18:0-C24:0. The ion at *m/z* 420.6 indicates Hex1-4Hex corresponding to Gb3Cer. The ion designations for ceramide and carbohydrate were assigned as described [12, 35]

Cers (d18:1-NFA types) [15]. Szulc *et al.* observed similar results using breast cancer cells MCF7 with synthetic Cers (d18:1-HFAs) [17]. In contrast, a less toxic effect of Cers with HFAs was reported in human leukemic cells U937 [23] and yeast cells [24]. The cytotoxicity of HFAs in Cers may depend on the cell types [11].

Under hypoxia, the proportion of species with d18:1 and/or HFAs was remarkably reduced with a concomitant increase in the proportion of the counterpart species with d18:0 and/or NFAs. These changes probably reflect the inability of dihydroceramide desaturase (DES) and fatty acid 2-hydroxylase to act in the hypoxic environment as these enzymes require molecular oxygen to function [11, 25]. Such decreases in the proportion of species with d18:1 tended to be considerable in Hex2Cers and Hex3Cers, but in HexCers, the proportion of HexCer (d18:1-C16:0) and HexCer (d18:1-C24:0h) actually increased.

It should be noted that re-exposure to O_2 induced the common Cers species, d18:1-C16:0, d18:1-C24:1 and d18:1-C24:0, which were still observed at 24 h after reoxygenation. Consequently ceramide composition of Cers and sphingomyelins was very similar (Fig. 6, upper two graphs). In HexCers, the proportion of d18:1 had largely returned to the level observed with normoxia (from 82 % to 76 %), but the proportion of HFA still remained low (from 72 % to 52 %), at 24h after reoxygenation (Fig. 7), suggesting that the fatty acid 2-hydroxylase in Caco-2 cells is less sensitive to reoxygenation to regain activity. In Hex2Cers, Hex3Cers, and HexNAcHex3Cers, the recovery of the proportions of d18:1 and HFA to normoxic levels, was slower than for HexCers, probably because of the time lag for synthesizing the GSLs by the sequential actions of glycosyltransferases [26]. Among the fatty acid species, C24:1h was the most influenced by hypoxia, because two oxygen-requiring enzymes are essential for its synthesis: stearoyl-CoA desaturase, which introduces a single double bond in the fatty acid [27] and a fatty acid 2-hydroxylase [11]. Cer d18:1-C24:1 absent in Cers at normoxia appears after reoxygenation. Newly synthesized d18:1-C24:1 may rapidly convert to Hex3Cer, HexNAcHex3Cer. Interestingly HexNAcHex3Cers contain a relatively high proportion of the constituent ceramide species of d18:1-C24:1 and d18:1-C24:1h (Fig. 6, bottom graph), even under hypoxia. Ceramide species specific elongation of the sugar chain has been previously reported, which may bestow a specific function on GSLs [28].

Previously we had expected to find a significant amount of phytosphingolipids in the Caco2-cells because the cells originated from human cancer in the intestine, which is known to contain a large amount of phytosphingolipids [29]. Actually, Caco-2 cells expressed *DES2* mRNA that encode a C-4 hydroxylase to synthesize phytosphingosine (data not shown) [30]. However, we did not find any phytosphingolipid from Caco-2 cells under any culture condition. Indeed, we found substantial amounts of phytosphingolipids in another human

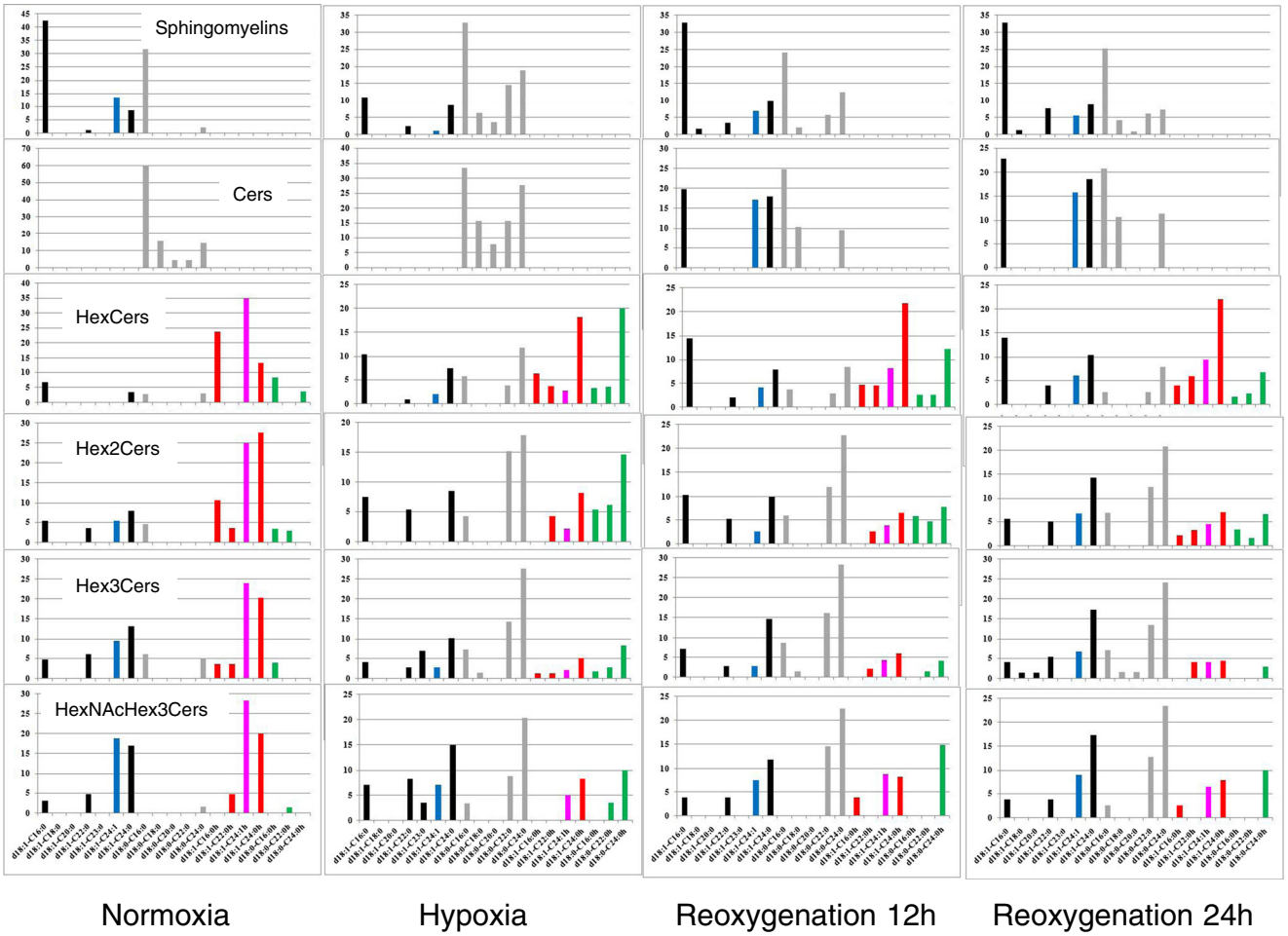

Fig. 6 Ceramide compositions of the sphingomyelins, Cers and NGSLs under normxia, hypoxia, and after reoxygenation for 12 and 24 h, respectively. Compositions were calculated based on the peak areas of the linear mass spectra. Black, gray, red, and green columns indicate species of d18:1-NFA, d18:0-NFA, d18:1-HFA, and d18:0-HFA, respectively. Blue and pink columns indicate species of d18:1-C24:1 and d18:1-C24:1h, respectively. Yaxis indicates percentage

colon cancer cell line LS174T, which brings more complexity to the analysis of sphingolipids in normoxia and hypoxia (unpublished data) because DES2 protein also requires molecular oxygen for its function.

The hydroxylation of FAs in the constituent ceramide species is known to affect the glycan functions of GSLs. Specifically, the hydroxylation of FA was reported to increase the antigenicity of the glycans [28] and to accelerate microbial adhesion to the host cells through the glycans of GSLs [31]. Although we expected that GSLs priorly use HFAs, it is surprising that GSLs also priorly use a common long-chain base of sphingosine (d18:1). Alteration of the glycans of GSLs in malignancy has been the subject of much investigation [32]. However, alteration of the constituent ceramide moieties of GSLs is also crucial for malignancy because malignant cancers are resistant to hypoxia [20] and GSLs tended to use sphinganine of d18:0 under a hypoxic condition. Investigation of ceramide moieties of GSLs, especially the significance of the trans-double bond in the long-chain base may reveal unexplored and promising targets for tumor therapy as those of Cers and sphingomyelins are currently ongoing [8, 9].

Finally we re-emphasize the characteristic distribution of the ceramide species according to the sphingolipid classes of Cers, sphingomyelins and NGSLs, not only in normoxic condition, but also hypoxic and the following reoxygenic conditions. Ceramide transfer protein (CERT) is well known to transport Cers in a non-vesicular manner from the endoplasmic reticulum to the Golgi apparatus for the synthesis of sphingomyelins, but whether CERT also transports Cers to the the Golgi apparatus for the synthesis of glucosylcermides (GlcCers) is controversial [33]. Recently, vesicular and non-vescular transport pathways for GlcCers in the Golgi apparatus have been elucidated [34]. The ceramide

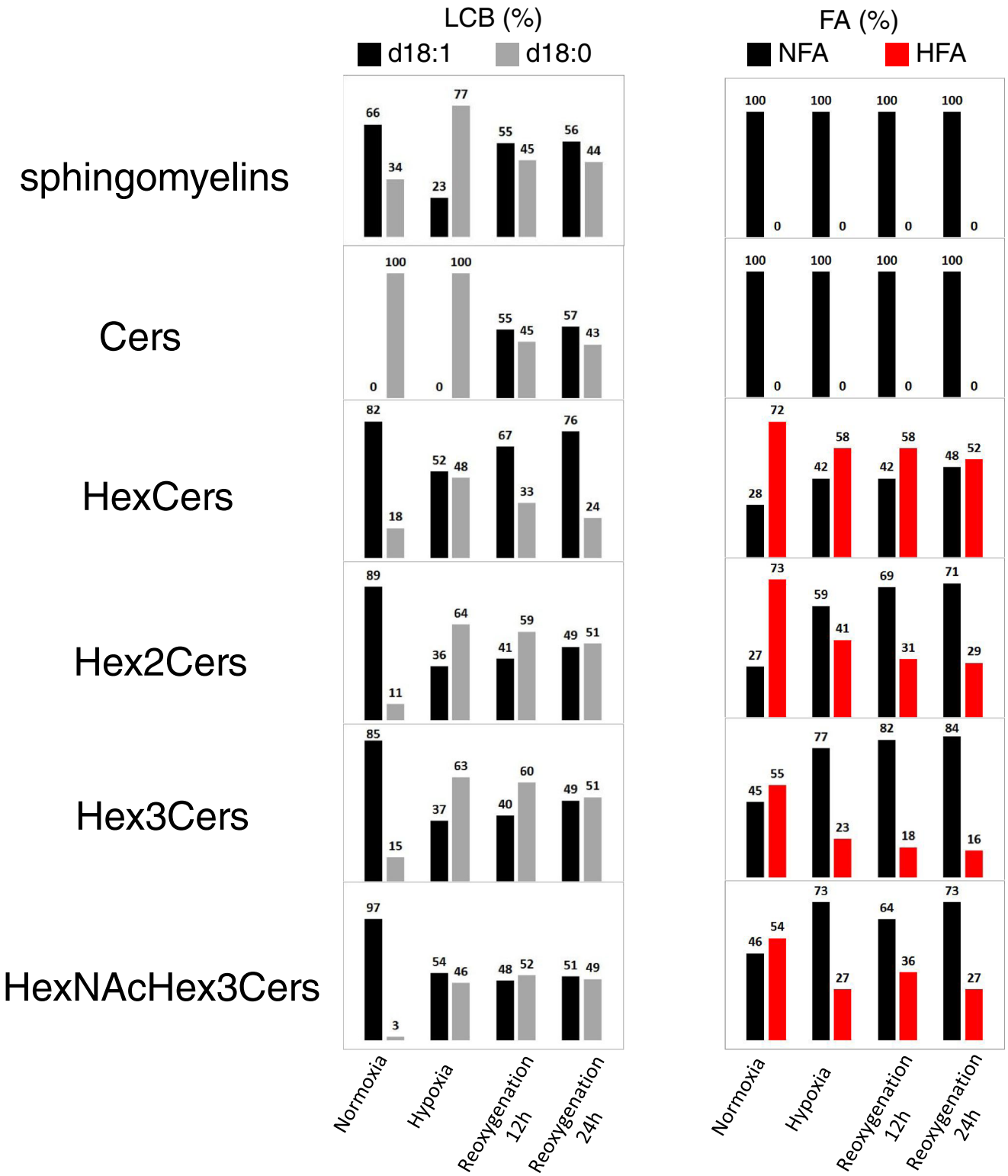

Fig. 7 Total composition of the long-chain base (LCB, *left* column) and FA (*right* column) in sphingomyelins, Cers, and NGSLs under normxia, hypoxia, and after reoxygenation for 12 and 24 h, respectively

portions of sphingolipids probably render profound effects on their membrane topology, so the differences of Cers and constituent ceramides of sphingolipids might also bestow considerable influences on the intracellular trafficking of sphingolipids, and resultantly their biological functions.

References

1. Merrill Jr., A.H.: Sphingolipid and glycosphingolipid metabolic pathways in the era of sphingolipidomics. Chem. Rev. **111**, 6387–6422 (2011)
2. Bielawski, J., Pierce, J.S., Snider, J., Rembiesa, B., Szulc, Z.M., Bielawska, A.: Comprehensive quantitative analysis of bioactive sphingolipids by high-performance liquid chromatography-tandem mass spectrometry. Methods Mol. Biol. **579**, 443–467 (2009)
3. Haynes, C.A., Allegood, J.C., Park, H., Sullards, M.C.: Sphingolipidomics: methods for the comprehensive analysis of sphingolipids. J. Chromatogr., B **877**, 2696–2708 (2009)
4. Grösch, S., Schiffmann, S., Geisslinger, G.: Chain length-specific properties of ceramides. Prog. Lipid Res. **51**, 50–62 (2012)
5. Buschard, K., Blomqvist, M., Månsson, J.E., Fredman, P., Juhl, K., Gromada, J.: C16:0 sulfatide inhibits insulin secretion in rat beta-cells by reducing the sensitivity of KATP channels to ATP inhibition. Diabetes **55**, 2826–2834 (2006)
6. Iwabuchi, K., Prinetti, A., Sonnino, S., Mauri, L., Kobayashi, T., Ishii, K., Kaga, N., Murayama, K., Kurihara, H., Nakayama, H., Yoshizaki, F., Takamori, K., Ogawa, H., Nagaoka, I.: Involvement of very long fatty acid-containing lactosylceramide in lactosylceramide-mediated superoxide generation and migration in neutrophils. Glycoconj J. **25**, 357–374 (2008)
7. Karahatay, S., Thomas, K., Koybasi, S., Senkal, C.E., Elojeimy, S., Liu, X., Bielawski, J., Day, T.A., Gillespie, M.B., Sinha, D., Norris, J.S., Hannun, Y.A., Ogretmen, B.: Clinical relevance of ceramide metabolism in the pathogenesis of human head and neck squamous cell carcinoma (HNSCC): attenuation of C(18)-ceramide in HNSCC tumors correlates with lymphovascular invasion and nodal metastasis. Cancer Lett. **256**, 101–111 (2007)
8. Signorelli, P., Munoz-Olaya, J.M., Gagliostro, V., Casas, J., Ghidoni, R., Fabriàs, G.: Dihydroceramide intracellular increase in response to resveratrol treatment mediates autophagy in gastric cancer cells. Cancer Lett. **282**, 238–243 (2009)
9. Fabrias, G., Muñoz-Olaya, J., Cingolani, F., Signorelli, P., Casas, J., Gagliostro, V., Ghidoni, R.: Dihydroceramide desaturase and dihydrosphingolipids: debutant players in the sphingolipid arena. Prog. Lipid Res. **51**, 82–94 (2012)
10. Deeley, J.M., Hankin, J.A., Friedrich, M.G., Murphy, R.C., Truscott, R.J., Mitchell, T.W., Blanksby, S.J.: Sphingolipid distribution changes with age in the human lens. J. Lipid Res. **51**, 2753–2760 (2010)
11. Hama, H.: Fatty acid 2-Hydroxylation in mammalian sphingolipid biology. Biochim. Biophys. Acta **1801**, 405–414 (2010)
12. Tanaka, K., Yamada, M., Tamiya-Koizumi, K., Kannagi, R., Aoyama, T., Hara, A., Kyogashima, M.: Systematic analyses of free ceramide species and ceramide species comprising neutral glycosphingolipids by MALDI-TOF MS with high-energy CID. Glycoconj J. **28**, 67–87 (2011)
13. Devlin, C.M., Lahm, T., Hubbard, W.C., Van Demark, M., Wang, K.C., Wu, X., Bielawska, A., Obeid, L.M., Ivan, M., Petrache, I.: Dihydroceramide-based response to hypoxia. J. Biol. Chem. **286**, 38069–38078 (2011)
14. Saito, T., Hakomori, S.I.: Quantitative isolation of total glycosphingolipids from animal cells. J. Lipid Res. **12**, 257–259 (1971)
15. Kyogashima, M., Tadano-Aritomi, K., Aoyama, T., Yusa, A., Goto, Y., Tamiya-Koizumi, K., Ito, H., Murate, T., Kannagi, R., Hara, A.: Chemical and apoptotic properties of hydroxy-ceramides containing long-chain bases with unusual alkyl chain lengths. J. Biochem. **144**, 95–106 (2008)
16. Kyogashima, M., Tamiya-Koizumi, K., Ehara, T., Li, G., Hu, R., Hara, A., Aoyama, T., Kannagi, R.: Rapid demonstration of diversity of sulfatide molecular species from biological materials by MALDI-TOF MS. Glycobiology **16**, 719–728 (2006)
17. Szulc, Z.M., Bai, A., Bielawski, J., Mayroo, N., Miller, D.E., Gracz, H., Hannun, Y.A., Bielawska, A.: Synthesis, NMR characterization and divergent biological actions of 20-hydroxy-ceramide/dihydroceramide stereoisomers in MCF7 cells. Bioorg. Med. Chem. **18**, 7565–7579 (2010)
18. Rylova, S.N., Somova, O.G., Zubova, E.S., Dudnik, L.B., Kogtev, L.S., Kozlov, A.M., Alesenko, A.V., Dyatlovitskaya, E.V.: Content and structure of ceramide and sphingomyelin and sphingomyelinase activity in mouse hepatoma-22. Biochemistry (Mosc). **64**, 437–441 (1999)
19. Dyatlovitskaya, E.V., Kandyba, A.G., Kozlov, A.M., Somova, O.G.: Sphinganine in Sphingomyelins of tumors and mouse regenerating liver. Biochemistry (Mosc). **66**, 502–504 (2001)
20. Semenza, G.L.: Hypoxia, clonal selection, and the role of HIF-1 in tumor progression. Crit. Rev. Biochem. Mol. Biol. **35**, 71–103 (2000)
21. Svensson, M., Lindstedt, R., Radin, N.S., Svanborg, C.: Epithelial glucosphingolipid expression as a determinant of bacterial adherence and cytokine production. Infect. Immun. **62**, 4404–4410 (1994)
22. Kyogashima, M., Taketomi, T.: Lipids from human platelets in primary thrombocythemia. Jpn. J. Exp. Med. **56**, 113–118 (1986)
23. Ji, L., Zhang, G., Uematsu, S., Akahori, Y., Hirabayashi, Y.: Induction of apoptotic DNA fragmentation and cell death by natural ceramide. FEBS Lett. **358**, 211–214 (1995)
24. Tani, M., Kuge, O.: Hydroxylation state of fatty acid and long-chain base moieties of sphingolipid determine the sensitivity to growth inhibition due to AUR1 repression in Saccharomyces cerevisiae. Biochem. Biophys. Res. Commun. **417**, 673–678 (2012)
25. Michel, C., van Echten-Deckert, G., Rother, J., Sandhoff, K., Wang, E., Merrill Jr., A.H.: Characterization of ceramide synthesis. A dihydroceramide desaturase introduces the 4,5-trans-double bond of sphingosine at the level of dihydroceramide. J. Biol. Chem. **272**, 22432–22437 (1997)
26. Stanley, P.: Golgi glycosylation. Cold Spring Harb Perspect Biol. (2011) 3(4). doi:10.1101/cshperspect.a005199
27. Miyazaki, M., Ntambi, J.M.: Fatty acid desaturation and chain elongation in mammals. In: Vance, D.E., et al. (eds.) Biochemistry of lipids, lipoproteins and membranes, 5th edn, pp. 191–211. Elsevier, Amsterdam (2008)
28. Kannagi, R., Stroup, R., Cochran, N.A., Urdal, D.L., Young Jr., W.W., Hakomori, S.: Factors affecting expression of glycolipid tumor antigens: influence of ceramide composition and coexisting glycolipid on the antigenicity of gangliotriaosylceramide in murine lymphoma cells. Cancer Res. **43**, 4997–5005 (1983)
29. Nishimura, K.: Phytosphingosine is a characteristic component of the glycolipids in the vertebrate intestine. Comp Biochem Physiol B. **86**, 149–154 (1987)
30. Omae, F., Miyazaki, M., Enomoto, A., Suzuki, M., Suzuki, Y., Suzuki, A.: DES2 protein is responsible for phytoceramide biosynthesis in the mouse small intestine. Biochem. J. **379**, 687–695 (2004)
31. Strömberg, N., Karlsson, K.A.: Characterization of the binding of Actinomyces naeslundii (ATCC 12104) and Actinomyces viscosus (ATCC 19246) to glycosphingolipids, using a solid-phase overlay approach. J. Biol. Chem. **265**, 11251–11258 (1990)
32. Hakomori, S.: Tumor-associated carbohydrate antigens defining tumor malignancy: basis for development of anti-cancer vaccines. Adv. Exp. Med. Biol. **491**, 369–402 (2001)
33. Hanada, K.: Intracellular trafficking of ceramide by ceramide transfer protein. Proc Jpn Acad Ser B Phys Biol Sci. **86**, 426–437 (2010)
34. D'Angelo, G., Uemura, T., Chuang, C.C., Polishchuk, E., Santoro, M., Ohvo-Rekilä, H., Sato, T., Di Tullio, G., Varriale, A., D'Auria, S., Daniele, T., Capuani, F., Johannes, L., Mattjus, P., Monti, M., Pucci, P., Williams, R.L., Burke, J.E., Platt, F.M., Harada, A., De Matteis, M.A.: Vesicular and non-vesicular transport feed distinct glycosylation pathways in the Golgi. Nature **501**, 116–120 (2013)
35. Domonand, B., Costello, C.E.: A systematic nomenclature for carbohydrate fragmentations in FAB-MS/MS spectra of glycoconjugates. Glycoconj. J. **5**, 397–409 (1988)